

Unravelling the Origin of the High-Catalytic Activity of Supported Au: A Density-Functional Theory-Based Interpretation

Norge Cruz Hernández,[†] Javier Fdez. Sanz,^{*,†} and José A. Rodríguez[‡]

*Departamento de Química Física, Facultad de Química, Universidad de Sevilla, E-41012 Sevilla, Spain, and
Department of Chemistry, Brookhaven National Laboratory, Upton, New York 11973*

Received October 4, 2006; E-mail: sanz@us.es

Gold is considered a rather inert metal in its bulk form; however, it can exhibit unexpectedly catalytic activity when it is highly dispersed on metal oxides.^{1,2} CO oxidation catalyzed by supported gold has been investigated in detail for both its simplicity and its technological importance.^{3–8} The outstanding activity of supported gold particles has been attributed to structural effects as size, shape, and thickness, as well as to support effects. In particular, it is observed that Au supported on reducible oxides, such as TiO₂, has a higher reactivity compared to Au on irreducible oxides, such as MgO and SiO₂.⁵

A few theoretical papers have been devoted to the microscopic aspects of CO oxidation by supported gold catalysts.^{9–12} The potential reactivity of different sites of gold cluster models deposited on TiO₂ and MgO has been examined using density-functional theory (DFT) calculations. The general conclusion of these DFT calculations is that the edge of the Au/support interface plays a key role in the mechanism of CO oxidation. However, in spite of all these efforts, the basic grounds of the oxidation mechanism still are far from being understood.

Concerning the structure of the catalysts, Goodman et al. experimentally found that two-layer Au particles supported on TiO₂ have the highest activity.³ In a more recent experiment, Cheng and Goodman reported well-ordered Au monolayers and bilayers that completely wet the oxide support, thus eliminating particle shape and direct support effects.⁴ In these systems the catalytic oxidation of carbon monoxide was studied and showed an unprecedented activity for a Au partially bilayered structure (more than an order of magnitude higher with respect to the monolayer). The catalyst was prepared by dispersing Au on a TiO_x film deposited on a Mo(112) surface.

That such a model catalyst precludes a direct contact with the support makes it of special interest in understanding the mechanism, and prompted us to perform a theoretical study based on periodic DFT calculations using a slab model. For this purpose we used the projected augmented wave VASP code¹³ and a plane-wave basis set. Two different functionals were used, the revised Perdew–Burke–Ernzerhof (RPBE)¹⁴ and the Perdew–Wang-91 (PW91).¹⁵

To model the Au/TiO_x/Mo(112) catalysts, we started from a Mo slab initially represented by a rectangular three-layer thick supercell of Mo(112)–(1 × 1) with *a* = 4.450 and *b* = 2.725 Å. The separation of the slabs was 15 Å to prevent interslab interactions. After relaxation of such a slab, we deposited a layer of titanium and oxygen atoms and looked for the different patterns that can accommodate the film. Our calculations showed that only a Ti₂O₃ stoichiometry was able to reproduce the (8 × 2) LEED pattern observed by Goodman et al.⁴ In this surface, for every eight Mo atoms, there are seven Ti atoms directly bonded to the Mo support. The shortest Ti–Ti distance is 3.115 Å. The O atoms bridge the

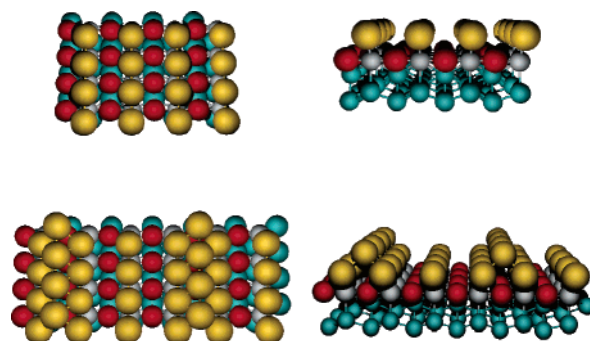


Figure 1. Optimized structures for Au deposited on TiO–Mo(112) surfaces: top, 1 ML; bottom, $\frac{4}{3}$ ML; Au, yellow; Ti, gray; Mo, blue; O, red.

Ti atoms forming two rows along the $[\bar{1}\bar{1}1]$ direction. One O row lies on the same plane as the Ti atoms, and the other is slightly protruded.

Addition of Au atoms to this Ti₂O₃/Mo(112) surface gives place to a relatively disordered monolayer close to the fcc (111) face; however, we were unable to find the (1 × 1) pattern that has been experimentally observed by Goodman et al. after annealing to 900 K gold particles dispersed on Mo(112)–(8 × 2)–TiO_x.⁴ Although we also considered structures arising after supporting Au on TiO₂/Mo(112) model surfaces, we found that the (1 × 1) pattern could only be reproduced if the titanium oxide stoichiometry was TiO. The structure of the surface model corresponding to 1 ML coverage of gold on TiO/Mo(112)–(1 × 1) is reported in Figure 1 (top). The geometry optimization shows that the most stable site for gold atoms is on Ti–Ti bridges, the Ti–Au distance being 2.711 Å. Notice that the Au–Au interatomic distance (2.725 Å), which is imposed by the Mo lattice, is significantly shorter than the bulk value (2.88 Å). Further gold addition to this monolayer leads to a model with coverage of $\frac{4}{3}$ ML (Figure 1, bottom) whose structure is consistent with the 1 × 3 LEED pattern reported Goodman et al.⁴ for this coverage. In this structure, overlayer gold atoms lie at the hollow sites, with a Au(first-layer)–Au(second-layer) distance of 2.897 Å.

The CO molecule readily adsorbs on the Au/TiO/Mo(112) surface, the largest adsorption energies being 0.39, 0.66, and 0.62 eV for 1, $\frac{4}{3}$, and $\frac{5}{2}$ ML coverage, respectively. These values are in quite good agreement with the data of Meier and Goodman¹⁶ who reported a CO binding energy of 0.8 eV on TiO₂ supported Au bilayers. For 1 and $\frac{5}{2}$ ML, the bridge sites in which CO binds two Au atoms appear to be more stable while the opposite is found for $\theta = \frac{4}{3}$ ML, where the on-top sites are preferred, the first (isolated row) Au atoms being slightly favored with respect to the topmost ones (0.57 eV), in agreement with the IRAS data reported by Chen et al.¹⁹ In both cases the CO molecule is noticeably tilted. On the other hand, molecular oxygen adsorption is energetically

[†] Universidad de Sevilla.

[‡] Brookhaven National Laboratory.

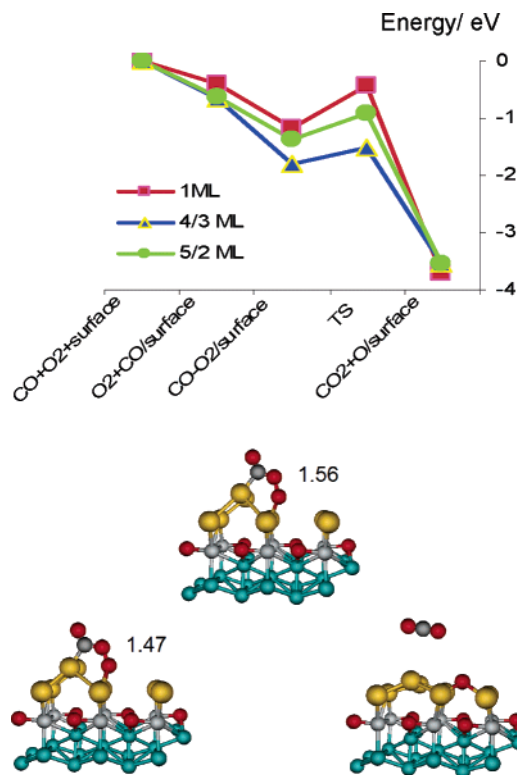


Figure 2. Top: Energy profiles for CO oxidation on Au/TiO–Mo(112) surface. Bottom: Structure of the peroxo-type CO–O₂ complex (left), transition state (middle), and final state (right) for CO oxidation on the ⁴/₃ Au/TiO–Mo(112) surface.

disfavored in all sites we explored on both the CO-free and the CO-covered surfaces. However, adsorbed CO is able to capture an oxygen molecule to give formation of a CO–O₂ intermediate complex (Figure 2). The formation of this peroxo-type complex is in agreement with the experimental data reported by Huber et al.¹⁷ as well as with the theoretical findings of Molina et al. on the Au/MgO catalyst.⁹ Using a 2 × 2 cell to avoid side intercell interactions, the formation energy of this complex with respect to gas O₂ and adsorbed CO is computed to be 0.62–0.78 eV, very close to the values reported by Molina et al. In this complex the terminal peroxide oxygen atom is also bound to nearby Au surface atoms, with Au–O distances ranging between 2.23 and 2.38 Å.

Starting from these peroxo-type complexes, we performed a transition state search using the nudge elastic-band approach and estimated the activation energies for the O–O dissociation giving rise to CO₂, which desorbs, and one oxygen atom that remains bound onto nearby Au atoms. The estimated barriers using the RPBE functional are 0.74, 0.29, and 0.45 eV for coverage of 1, ⁴/₃, and ⁵/₂ ML, respectively. The outstanding result here obviously is the significant lowering of the barrier for the (1 × 3) structure for which the oxygen activation appears to occur much more easily.

On the other hand, the remaining atomic oxygen on the surface, which has been shown to be highly reactive would promptly oxidize further incoming CO.¹⁸

The key structural differences between the 1 ML or the ⁵/₂ ML Au catalysts and the highly reactive ⁴/₃ ML case relies on the two layers of Au involved in the reaction. In the latter structure, O atoms are bound to bottom Au atoms which are directly sitting on partially oxidized Ti atoms, while CO is adsorbed on top of undercoordinated Au atoms of the top layer. It appears that this structural arrangement gives place to a synergistic reaction as suggested by Chen et al.¹⁹ Our calculations show that around the bottom Au layer there is a larger electron density which would favor the charge transfer toward the antibonding pseudo-2π orbital of the peroxo-type fragment which obviously weakens the O–O bond and consequently leads to the oxygen activation.²⁰ The density of states, DOS, projected on the surface atoms shows at the top of the valence band clearly defined states arising from the mix of Au 5d and O₂ 2π orbitals.

Acknowledgment. This work was funded by the Spanish Ministerio de Educación y Ciencia and the European FEDER: Project MAT2005-01872. N.C.H. thanks the Ramón y Cajal program for a grant. We also thank the computer resources provided by the Barcelona Supercomputing Center—Centro Nacional de Supercomputación.

Supporting Information Available: Top and side views of the Mo(112)–(8 × 2)–Ti₂O₃ surface. This material is available free of charge via the Internet at <http://pubs.acs.org>.

References

- (1) Haruta, M. *Catal. Today* **1997**, *36*, 153.
- (2) Meyer, R.; Lemire, C.; Shaikuthdinov, S. K.; Freund, H.-J. *Gold Bull.* **2004**, *37*, 72–124.
- (3) Valden, M.; Lai, X.; Goodman, D. M. *Science* **1998**, *281*, 1647.
- (4) Chen, M. S.; Goodman, D. W. *Science* **2004**, *306*, 252.
- (5) Schubert, M.; Hackenberg, S.; van Veen, A. C.; Muhler, M.; Plzak, V.; Behm, R. J. *J. Catal.* **2001**, *197*, 113.
- (6) Grisel, R. J. H.; Nieuwenhuys, B. E. **2001**, *199*, 48.
- (7) Bondzie, V. A.; Parker, S. C.; Campbell, C. T. *J. Vac. Sci. Technol., A* **1999**, *17*, 1717.
- (8) Stampfl, C.; Scheffler, M.; *Phys. Rev. Lett.* **1997**, *78*, 1500.
- (9) López, N.; Nørskov, J. K. *J. Am. Chem. Soc.* **2002**, *124*, 11262.
- (10) Molina, L. M.; Hammer, B. *Appl. Catal., A* **2005**, *291*, 21 and references therein.
- (11) Liu, Z.-P.; Gong, X.-Q.; Kohanoff, J.; Sanchez, C.; Hu, P. *Phys. Rev. Lett.* **2003**, *91*, 266102.
- (12) Remediakis, I. N.; Lopez, N.; Nørskov, J. K. *Angew. Chem., Int. Ed.* **2005**, *44*, 1824.
- (13) Kresse, G.; Furthmüller, J. *Phys. Rev. B: Condens. Matter Mater. Phys.* **1996**, *54*, 11169.
- (14) Hammer, W.; Hansen, L. B.; Nørskov, J. K. *Phys. Rev. B: Condens. Matter Mater. Phys.* **1999**, *59*, 7413.
- (15) Perdew, J.; Chevary, J.; Vosko, S.; Jackson, K.; Pederson, K.; Singh, D.; Fiolhais, C. *Phys. Rev. B: Condens. Matter Mater. Phys.* **1992**, *46*, 6671.
- (16) Meier, D. C.; Goodman, D. W. *J. Am. Chem. Soc.* **2005**, *126*, 1892.
- (17) Huber, H.; McIntosh, D.; Ozin, G. A. *Inorg. Chem.* **1997**, *16*, 975.
- (18) Stiehl, J. D.; Gong, J.; Ojifinni, R. A.; Kim, T. S.; McClure, S. M.; Mullins, C. B. *J. Phys. Chem. B* **2006**, *110*, 20337.
- (19) Chen, M. S.; Cai, Y.; Yan, Z.; Goodman, D. W., *J. Am. Chem. Soc.* **2006**, *128*, 6341.
- (20) Yoon, B.; Häkkinen, H.; Landman, U. *J. Phys. Chem. B* **2003**, *107*, 4066.

JA0670153